National Conference with International Participation

ENGINEERING MECHANICS 2008

Svratka, Czech Republic, May 12 – 15, 2008

AN ANALYSIS OF INERTIA AND STIFFNESS PROPERTIES OF DAMAGED SHELL ELEMENT

Š. Fenik*, L. Starek**

Summary: *Vibration-based damage detection methods are usualy based on comparison of the natural frequencies and mode shapes of test structure gained by experimental modal analysis with their analytical counterparts computed using FEM model. In this context the modelling method of damaged region plays key role in parametric methods of damage detection. This paper is concerned with the modelling of the shell element damaged by line crack. The main idea lies in using detailed finite subelement modelling of the damaged shell element and subsequent reduction of element mass and stiffness matrices. Changes in inertia and stiffness properties of damaged shell element are closely analyzed and simulated example of damage detection is presented for comparison of matrix reduction method with classical method of damage modelling, i.e. change of Young's modulus in damaged element.*

1. Introduction

It is well known that even slight cracks or small damages can influence the dynamic behaviour of mechanical structure at significant level. Since this behaviour can be described by means of the modal system parameters, changes in inertia and stiffness properties of structure will induce an appropriate change in natural frequencies and mode shapes. This fact together with the need of non-destructive global techniques for structure diagnosis has led to the continuous development of variety of so called vibration-based damage detection methods in a few past decades (see Yan et al. (2006) or Doebling et al. (1998) for review).

In recent past growing attention is paid to plate-like structures which are very important in aerospace, automotive and civil engineering. In comparison with beam-like structures the damage detection of plates and shells is more complex problem in the field of experimental modal analysis as well as in the field of simulations and mathematical modelling. In present works two simple types of crack are usually considered: (1) **reduction of stiffness** (e.g. Cornwell et al., 1999, Bayissa & Haritos, 2007) and (2) **reduction of thickness** of given damaged area within one or more finite shell elements (e.g. Yam et al., 2002). In general, the changes in inertia properties are not considered.

* Ing. Štefan Fenik, PhD.: Faculty of Mechanical Engineering, Slovak University of Technology, Nám. slobody 17; 812 31 Bratislava, Slovakia; tel.: +421 257 296 479; e-mail: stefan.fenik@stuba.sk

** Prof. Ing. Ladislav Starek, PhD.: Faculty of Mechanical Engineering, Slovak University of Technology, Nám. slobody 17; 812 31 Bratislava, Slovakia; tel.: +421 257 296 327; e-mail: ladislav.starek@stuba.sk

This work has the aim of analysing the both inertia and stiffness properties of the shell element with line crack by the means of reduced mass and stiffness element matrices. Several crack situations with various positions are analysed using Finite Element Method (FEM). Results are presented graphically and derived matrices are used in simulated example of damage detection of free rectangular plate.

2. Mathematical description

Suppose that we have damaged rectangular plate divided into regular mesh of shell elements, where the length of crack is relatively small in comparison with the dimension of the mesh. In such case the reduction of stiffness or thickness of the whole element is not sufficient for locating the crack thus more detailed modelling is needed. For further analysis purposes, the damaged area, identical with appropriate FEM model element, can be modelled as rectangular plate divided into subelements, where corner nodes represent the nodes of considered damaged shell element. Crack or damage is modelled as discontinuity of the connection between neighbouring elements in appropriate node(s) as it is shown in Fig. 1.

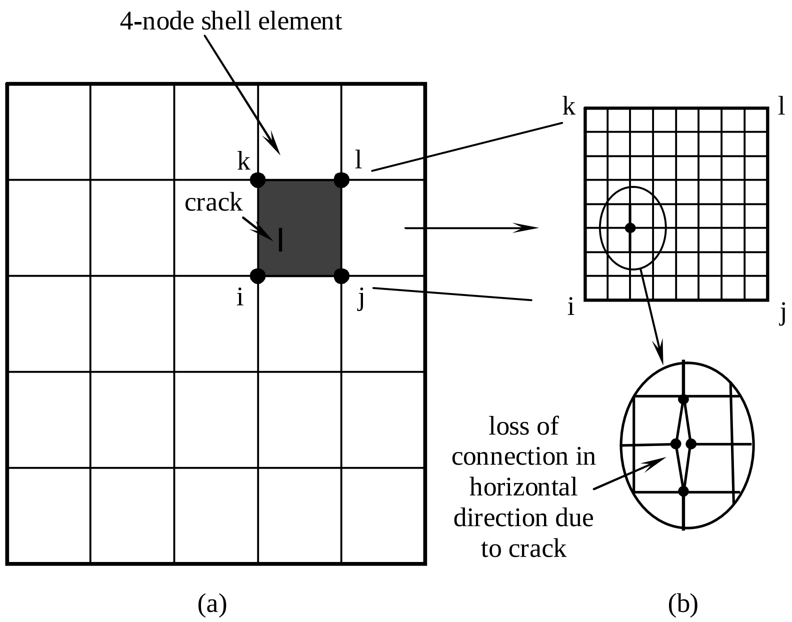

Fig. 1: Shell element with crack: a) plate divided into rectangular elements b) FEM model of the element with line crack

Desired mass and stiffness matrices of the element, in local coordinate system, can be derived by computation of reaction forces in subsequent analyses of distinct unit kinematic loads within all desired degrees of freedom (DOF), which are the out-of-plane deflection and rotations about in-plane axes, i.e. 3 DOFs per node, 12 DOF per element (in-plane deformations are irrelevant). In fact, this is computation of some kind of reduced FEM matrices, where master DOFs are the out-of-plane deflections and rotations in corner nodes *i*, *j*, *k*, *l*. Equation of motion for full model of the element in case of harmonic load is:

$$\mathbf{M}\ddot{\mathbf{q}} + \mathbf{K}\mathbf{q} = \mathbf{f}e^{j\omega t} \tag{1}$$

where $\mathbf{M}$, $\mathbf{K}$ are mass and stiffness matrices of the element for full mesh (Fig. 1b), $\mathbf{q}$ is corresponding displacement vector, $\mathbf{f}$ is vector of force amplitudes and ω is driving frequency.

Let $\mathbf{q}_m$ be the master DOFs amplitude vector and let $\mathbf{q}_s$ represent amplitudes of the remaining DOFs (i.e. slaves). Now assuming the harmonic response, equation of motion (1) can be expressed in block-matrix form:

$$\left(-\omega^2\begin{bmatrix}\mathbf{M}_{mm} & \mathbf{M}_{ms}\\ \mathbf{M}_{sm} & \mathbf{M}_{ss}\end{bmatrix}+\begin{bmatrix}\mathbf{K}_{mm} & \mathbf{K}_{ms}\\ \mathbf{K}_{sm} & \mathbf{K}_{ss}\end{bmatrix}\right)\begin{bmatrix}\mathbf{q}_m\\ \mathbf{q}_s\end{bmatrix}=\begin{bmatrix}\mathbf{f}_m\\ \mathbf{0}\end{bmatrix} \tag{2}$$

where $\mathbf{f}_m$ is vector of force amplitudes within master DOFs (while forces on slave DOFs are assumed to be zero).

From (2) we have following equation for $\mathbf{q}_s$:

$$\left(\mathbf{K}_{ss}-\omega^2\mathbf{M}_{ss}\right)\mathbf{q}_s=-\left(\mathbf{K}_{sm}-\omega^2\mathbf{M}_{sm}\right)\mathbf{q}_m \tag{3}$$

Using (3) we can write transformation formula for complete DOF vector $\mathbf{q}$:

$$\begin{bmatrix}\mathbf{q}_m\\ \mathbf{q}_s\end{bmatrix}=\mathbf{q}=\mathbf{T}(\omega)\mathbf{q}_m \quad \Rightarrow \quad \mathbf{T}(\omega)=\begin{bmatrix}\mathbf{I}\\ -\left(\mathbf{K}_{ss}-\omega^2\mathbf{M}_{ss}\right)^{-1}\left(\mathbf{K}_{sm}-\omega^2\mathbf{M}_{sm}\right)\end{bmatrix} \tag{4}$$

where $\mathbf{T}(\omega)$ is frequency-dependent transformation matrix.

Finally, reduced element matrices can be computed as:

$$\mathbf{M}_{red}=\mathbf{T}^T\mathbf{M}\mathbf{T} \quad \mathbf{K}_{red}=\mathbf{T}^T\mathbf{K}\mathbf{T} \tag{5a,b}$$

where $\mathbf{M}_{red}$, $\mathbf{K}_{red}$ are element mass and stiffness matrices reduced into local (i.e. master DOFs) coordinates $\mathbf{q}_m$.

For zero value of ω equations (5) represent static reduction (also known as Guyan). Making reduction of element matrices for undamaged and damaged case (see Fig. 1b) we can get representation of damage as difference between appropriate mass and stiffness matrices:

$$\mathbf{M}_{dmg}=\mathbf{M}_{red}^{d}-\mathbf{M}_{red} \qquad \mathbf{K}_{dmg}=\mathbf{K}_{red}^{d}-\mathbf{K}_{red} \tag{6}$$

where $\mathbf{M}_{red}^{d}$ is mass matrix for damaged element, $\mathbf{M}_{dmg}$ is “mass matrix” of the damage, $\mathbf{K}_{red}^{d}$ is stiffness matrix for damaged element, $\mathbf{K}_{dmg}$ is “stiffness matrix” of the damage.

Now the damage can be incorporated into the FEM model of the plate by the means of mass and stiffness matrices. First the matrices of damage (6) should be transformed to global coordinate system of the plate and then added to corresponding global matrices. Let $\mathbf{q}_g$ be the global coordinate vector and $\mathbf{R}$ the coordinate transformation matrix, containing partial derivations of local coordinates $\mathbf{q}_m$ with respect to global coordinates:

$$\mathbf{q}_m = \mathbf{R}\mathbf{q}_g \quad \Rightarrow \quad \mathbf{R} = \frac{\partial \mathbf{q}_m}{\partial \mathbf{q}_g^T} \tag{7}$$

It is clear that matrix $\mathbf{R}$ has non-zero values only for coordinates coupled with corner nodes of desired element. Finally the mass and stiffness matrices of damaged structure will be:

$$\mathbf{M}_g^d = \mathbf{M}_g + \mathbf{R}^T \mathbf{M}_{dmg} \mathbf{R} \qquad \mathbf{K}_g^d = \mathbf{K}_g + \mathbf{R}^T \mathbf{K}_{dmg} \mathbf{R} \tag{8}$$

where $\mathbf{M}_g^d$ is global mass matrix of the structure with damage (crack), $\mathbf{M}_g$ is mass matrix of undamaged plate, $\mathbf{K}_g^d$ is global stiffness matrix of the structure with damage, $\mathbf{K}_g$ is stiffness matrix of undamaged plate.

3. Analysis of the shell element with line crack

In this section we will analyse inertia and stiffness properties of chosen shell element, which is square element of width 100 *mm* and thickness 4 *mm*. Material of the element is irrelevant for relative results, in this example commercial aluminium was chosen. We use mesh 5 by 5 subelements for detailed modelling of this element. The length of crack we choose as three times the dimension of subelement, so for three neighbouring nodes (only internal) conection in direction perpendicular to the direction of crack is interrupted. Under such conditions we have total number of 16 different locations of the crack, i.e. 8 in both in-plane directions. Since it is hard to display and compare full matrices (of dimension 12 by 12) only diagonal terms are displayed as representatives. Figures 2 and 4 show percentual change of the diagonal terms of reduced mass matrices, computed using (5a), due to crack. Figures 3 and 5 show percentual change of the diagonal terms of reduced stiffness matrices, computed using (5b). Results are presented only for four independent locations, remaining locations are given by rotation of the element by 90, 180 and 270 degrees counter-clockwise and gives same results. On the left side there are diagrams showing the geometry of the damage and on the right side there are corresponding plots of percentual change in diagonal terms versus local coordinates, which are the out-of-plane deflection (in *z* direction) and rotations about in-plane axes (*x* and *y*). Results for coordinates of the same type are grouped together for easier comparison and readability. There are both static (Fig. 2 and 3) and dynamic (Fig. 4 and 5) reduction results presented. Value of circular frequency ω for dynamic reduction was chosen as 1885 $rad.s^{-1}$ (300 *Hz*) with respect to frequency band usually considered within engineering structures (1 – 1000 *Hz*).

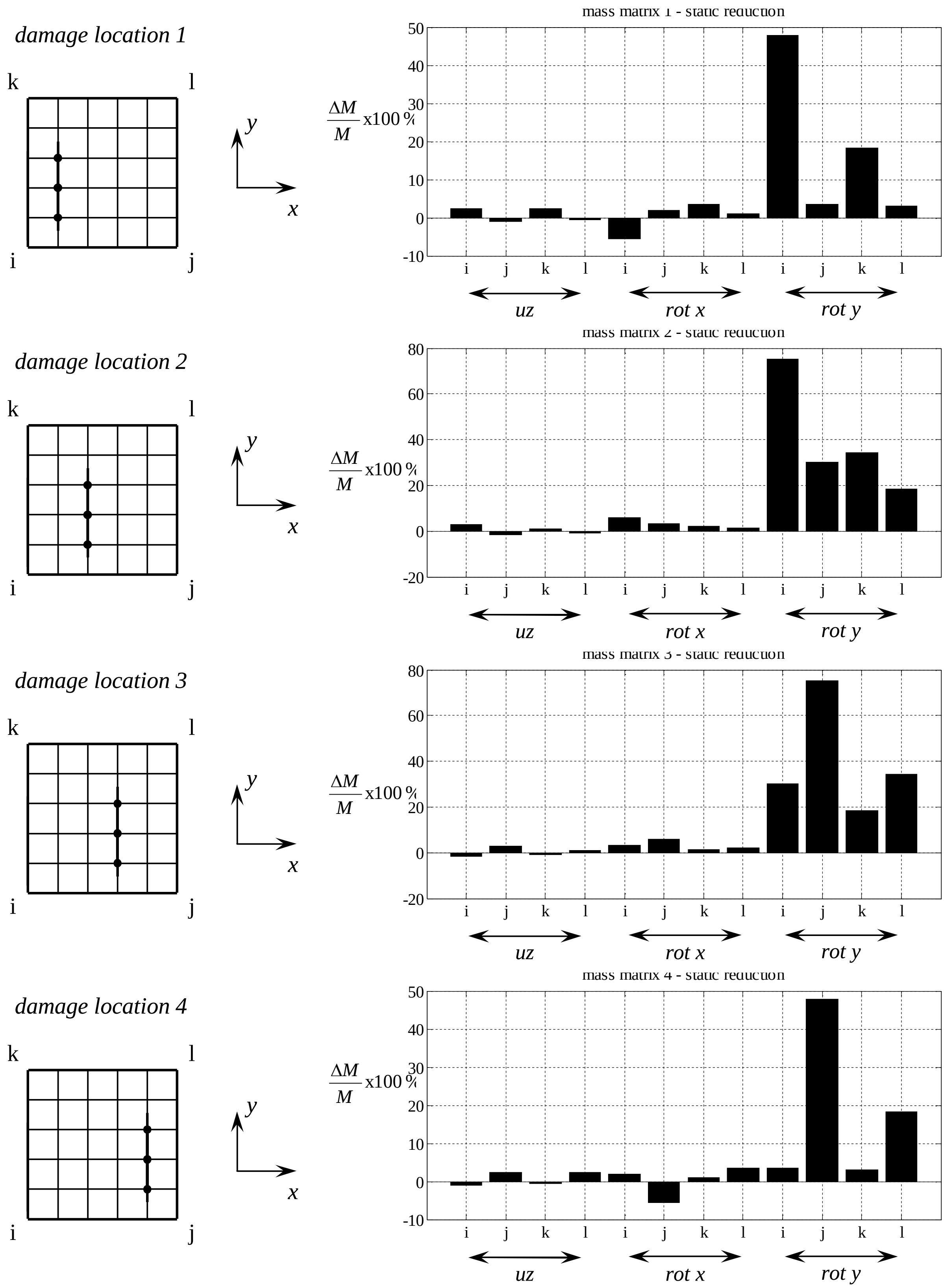

Fig. 2: Relative change of inertia due to line crack – static reduction

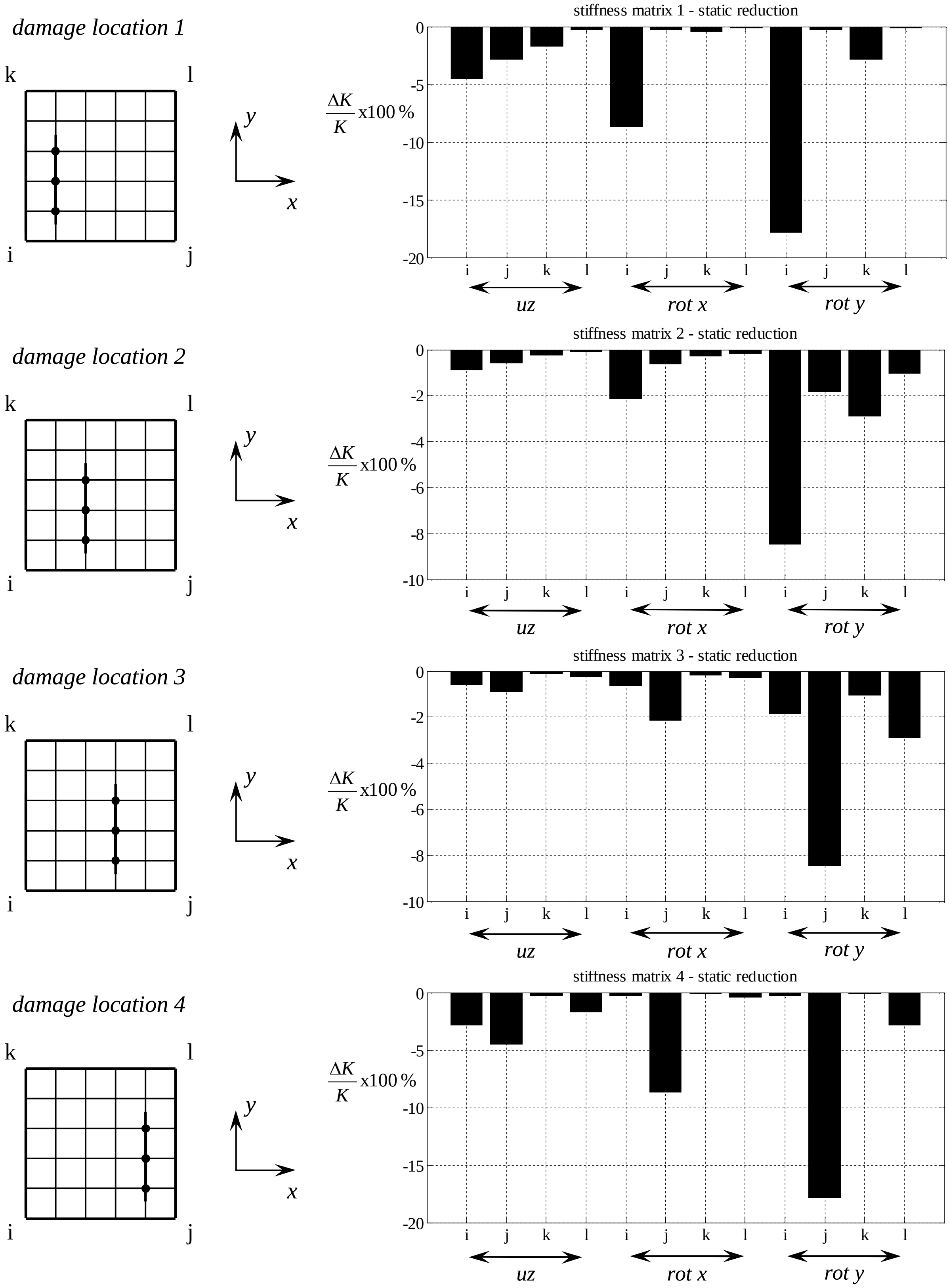

Fig. 3: Relative change of stiffness due to line crack – static reduction

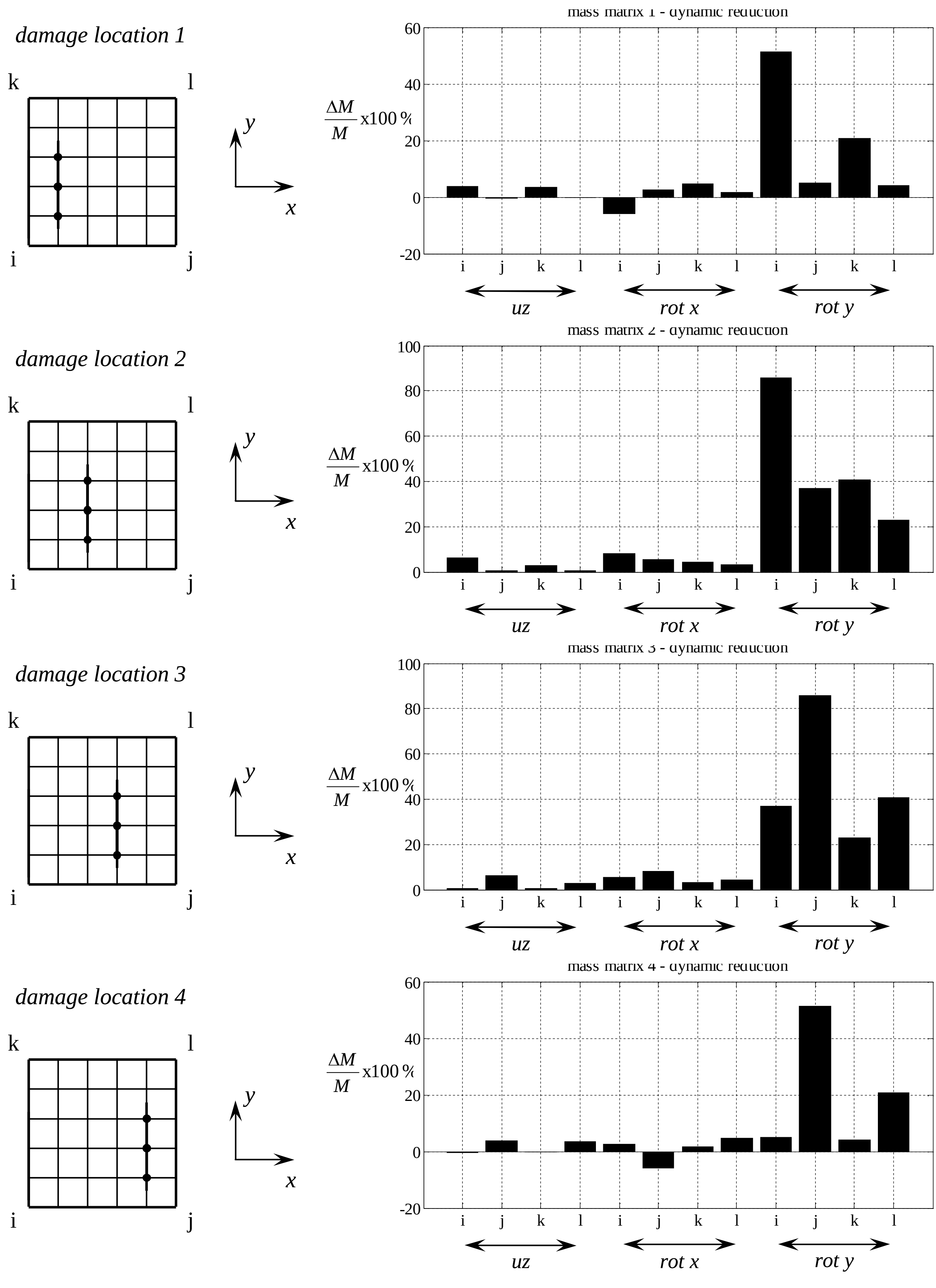

Fig. 4: Relative change of inertia due to line crack – dynamic reduction

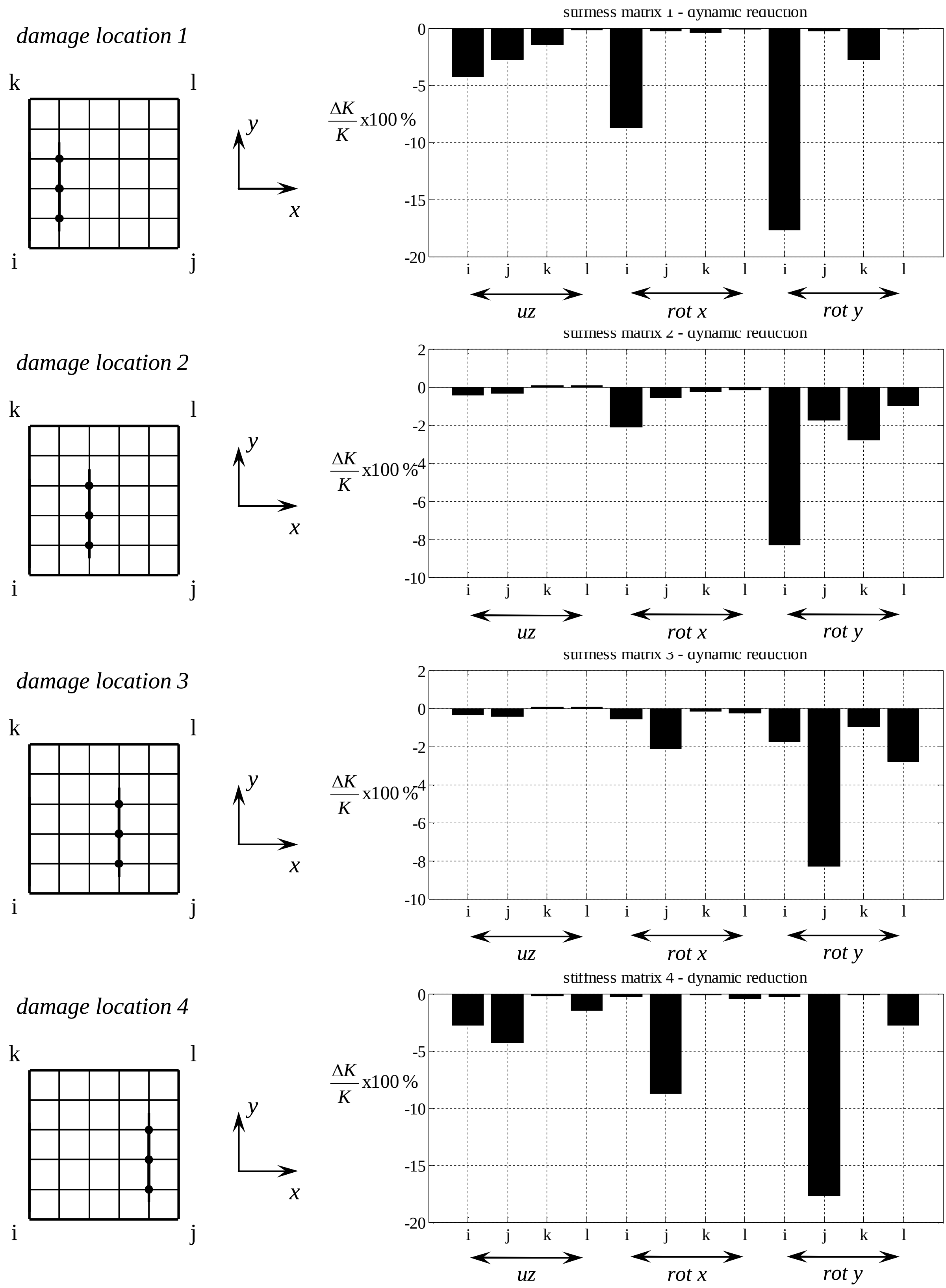

Fig. 5: Relative change of stiffness due to line crack – dynamic reduction

Analysis results can be summarized in following remarks:

- damage has negative influence on stiffness, but positive influence on inertia; this implicates decreasing tendency in natural frequencies of damaged structure
- dominant changes are in terms corresponding to rotation about axis parallel to direction of crack (i.e. *y* for locations 1 – 4)
- magnitude of property change is greater for node(s) located near the crack
- dynamic reduction (300 *Hz*) gives negligible differences in stiffness terms, but differences in inertia terms are significant (approx. +10%)
- maximum change in stiffness term is -18% within rotation about *y* axis in node *i* for location no. 1 (static reduction)
- maximum change in inertia is +85% within rotation about *y* axis in node *i* for location no. 2 (dynamic reduction)

4. Damage detection using reduced element mass and stifness matrices

Now let us demonstrate the advantages of using reduced element matrices in damage detection example. As a test structure we take 4 *mm* thick rectangular aluminium plate of dimensions 400 by 500 *mm*. Suppose we have identified the element where the damage is located and let it be the element no. 6 (see Fig. 6). Using detailed modelling of this element divided into 5 by 5 subelements we can get FEM model of the plate in the form (8), i.e. with damages of different dimensions and locations incorporated via reduced element matrices.

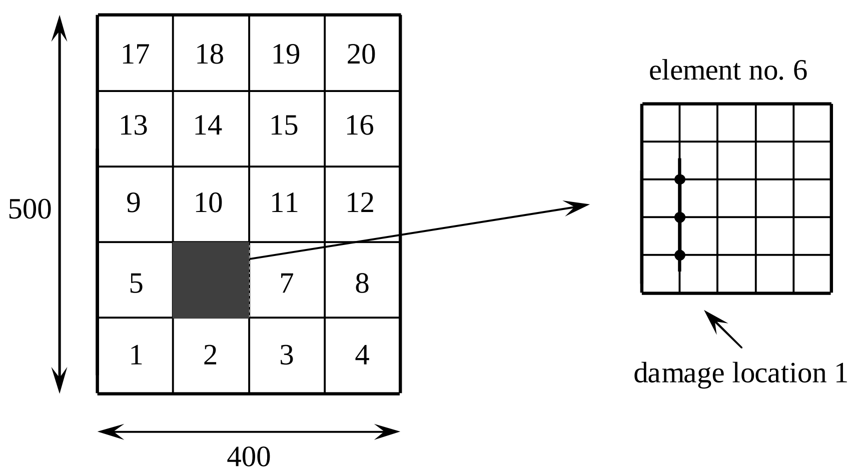

Fig. 6: Geometry of the damaged test plate

In the next step we compare experimental and analytical natural frequencies represented by changes within 10 lowest natural frequencies for different damage locations and also for the case of damage modelled as reduction of stiffness (Young's modulus) of the whole element. In our demonstration the experiment is simulated using FEM model of the plate with mesh of the density corresponding to the dimensions of subelements used for detailed modelling of the damaged element. This means the plate is divided into 20 by 25 elements and damage is modelled as discontinuity in chosen damage location (Fig. 6). Let Δf_{ex} be the diferencies in experimental natural frequencies:

$$\Delta f_{ex} = f_{exh} - f_{exd} \tag{9}$$

where f_{exh} is experimental natural frequency of healthy structure, f_{exd} is corresponding natural frequency of damaged structure.

Simulated experimental natural frequencies for healthy and damaged case are presented in Table 1:

Table 1: Simulated experimental natural frequencies (*Hz*)

mode	healthy f_{exh}	damaged f_{exd}	difference Δf_{ex}
1	64.876	64.861	-0.015
2	83.182	83.171	-0.011
3	139.67	138.16	-1.51
4	157.43	157.41	-0.02
5	184.83	184.33	-0.50
6	245.85	245.10	-0.75
7	307.59	307.37	-0.22
8	314.46	314.25	-0.21
9	378.20	370.75	-7.45
10	429.75	424.76	-4.99

Similarly we can compute the differencies in analytical natural frequencies for every considered damage location and compare them with the experimental results:

$$\Delta f_{an} = f_{anh} - f_{and} \tag{10}$$

where index *an* means analytical values corresponding to (9).

Figure 7 shows absolute difference between analytical and experimental frequencies versus 16 damage locations for 10 lowest modes in the case of static reduction. Figure 8 gives same kind of results for dynamic reduction (300 *Hz*). Results for dynamic reduction are slightly different but give same conclusion that the damage location no. 1 identifies the experimental one precisely.

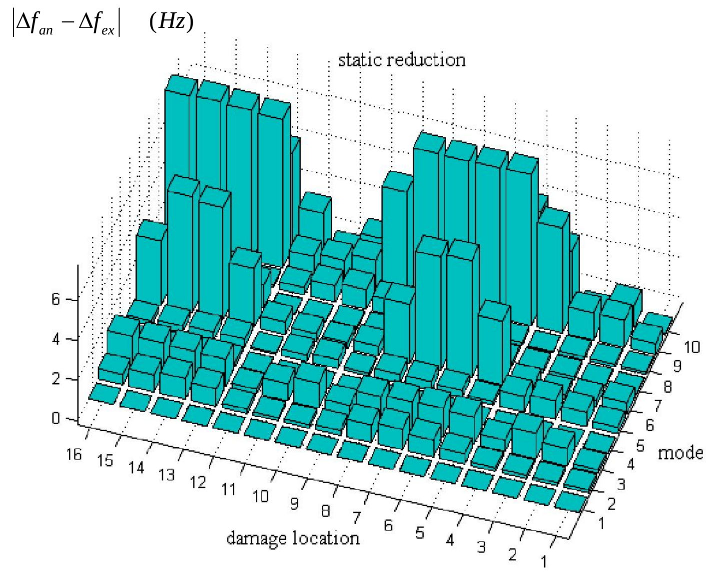

Fig. 7: Absolute changes of natural frequencies depending on damage location – static reduction

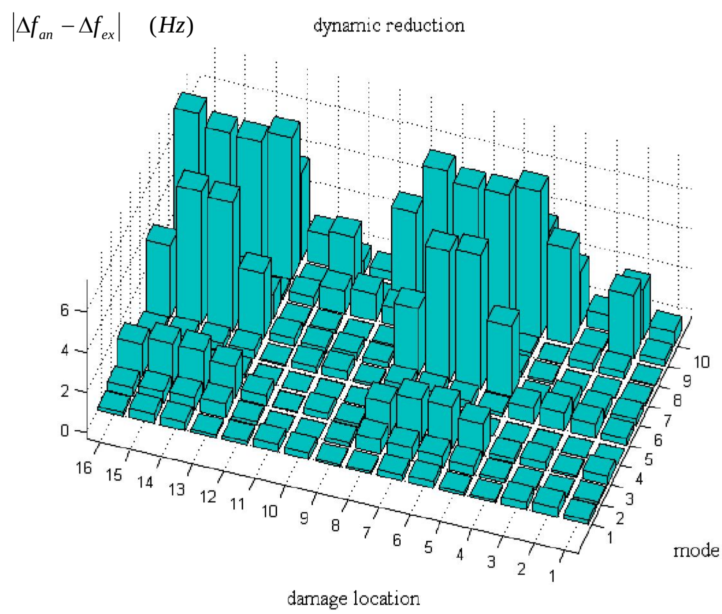

Fig. 8: Absolute changes of natural frequencies depending on damage location – dynamic reduction

Let us make comparison with the case when static reduction of stiffness matrix of the crack is used only, i.e. damage does not change the inertia properties. Figure 9 presents absolute differences between analytical and experimental frequencies versus 16 damage locations for 10 lowest modes in same manner as Fig. 7 and 8.

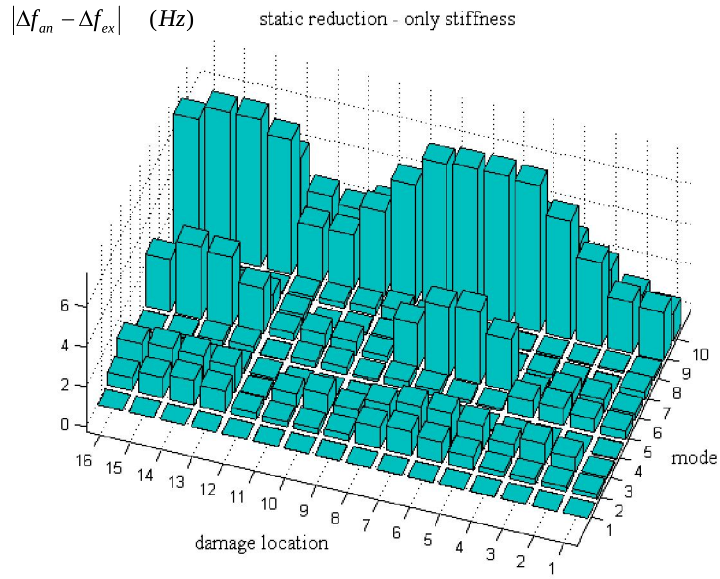

Fig. 9: Absolute changes of natural frequencies depending on damage location – only stiffness matrix considered

Using only stiffness of the damaged element we get significantly worse results, but the true position of the crack can be still uniquely determined.

For comparison with classical damage detection methods we compute natural frequencies for damaged element modelled with uniformly reduced stiffness (i.e. by change in Young's modulus for element no. 6). Figure 10 shows differences between analytical and experimental frequencies versus 10 values of Young's modulus ratio for 10 lowest modes. Best results are achieved for value 0.8 of the stiffness ratio; however, frequency changes can not match the experimental ones in no way.

For numerical evaluation we define following Frequency Difference Index (*FDI*), defined as Euclid norm of frequency changes within 10 lowest modes:

$$FDI = \sqrt{\sum_{i=1}^{10} \left(\Delta f_{an}(i) - \Delta f_{ex}(i)\right)^2} \tag{11}$$

where *i* is mode number.

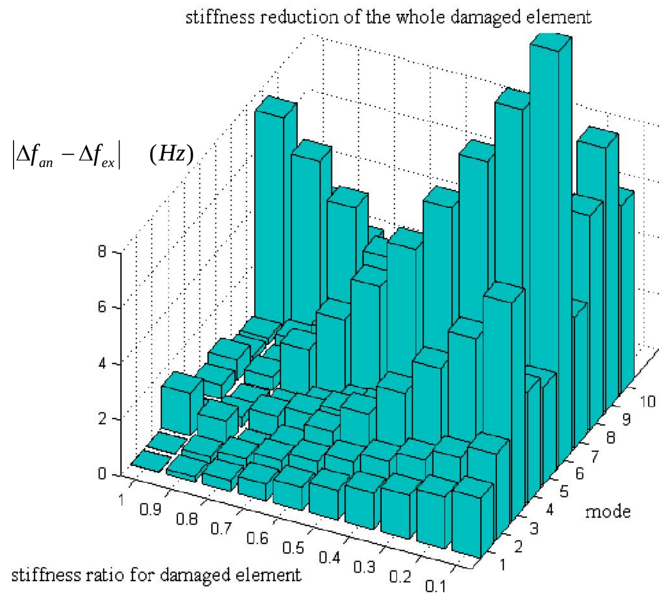

Fig. 10: Absolute changes of natural frequencies – damage modelled as stifness reduction in damaged element

In Table 2 computed values of *FDI* are summarized for previously analyzed cases.

Table 2: Frequency difference index (*Hz*) for damage detection

damage location	static reduction	dynamic reduction	stiffness matrix only
1	0.89	1.04	2.85
2	2.12	4.14	3.4
3	2.15	1.44	5.3
4	6.17	5.5	7.1
5	9.6	9.3	9.1
6	10.6	10.3	9.7
7	10.6	10.3	9.8
8	9.6	9.3	9.3
9	6.5	5.9	7.4
10	2.70	1.57	5.6
11	1.78	3.18	4.1
12	2.44	1.75	4.3
13	9.5	9.2	8.8
14	10.5	10.0	9.7
15	10.5	10.1	9.7
16	9.5	9.2	8.3

One can see that dynamic reduction gives no improvement in detection of the true damage location. Regardless on the type of matrix reduction, value of *FDI* is reliable indicator of the true location of the damage and can be recommended for use in damage detection. Also it is clear that inertia effect is important in damage detection and can not be neglected (as it can be seen from the third column of Table 2).

5. Conclusions

New approach in damage modelling of plate-like structures has been introduced which is capable to match the changes in modal properties more precisely then classical methods like stiffness and thickness reduction. Main feature of this method is the possibility of modelling true geometry of damage in the case of line crack. Using static or dynamic reduction of element matrices the damage can be easily incorporated into simplified FEM model with both inertia and stiffness properties considered in good agreement with full FEM model.

Simulated example of damage detection has shown the idea of matrix reduction to be well-founded. The best results were achieved for static reduction of stiffness and mass matrices. It has also been proved that change in inertia of the damaged element plays important role and can not be neglected. In the case of line crack the classical methods of damage modelling give significantly worse results in comparison with proposed matrix reduction method.

Acknowledgement

The paper was written with the support of APVV grant No. 20 – 063105

References

Bayissa, W. L. & Haritos, N. (2007) Structural damage identification in plates using spectral strain energy analysis, *Journal of Sound and Vibration*, 307, pp. 226 – 249

Cornwell, P., Doebling, S. W. & Farrar, C. R. (1999) Application of the Strain Energy Damage Detection Method to Plate-like Structures, *Journal of Sound and Vibration*, 224, 2, pp. 359 – 374

Doebling, S. W., Farrar, C. R. & Prime, M. B. (1998) A summary review of vibration-based damage identification methods. *The Shock and Vibration Digest* 30, 2, pp. 91 – 105

Yam, L. H., Li, Y. Y. & Wong, W. O. (2002) Sensitivity studies of parameters for damage detection of plate-like structures using static and dynamic approaches, *Engineering Structures*, 24, pp. 1465 – 1475

Yan, Y. J., Cheng, L., Wu, Z. Y. & Yam, L. H. (2006) Development in vibration-based structural damage detection technique, *Mechanical Systems and Signal Processing*, 21, pp. 2198 – 2211